INVITED PAPER *Special Section on Electronic Displays*

# Synthesis and Photoluminescence Properties of $HEu_{1-x}Gd_x(MoO_4)_2$ Nanophosphor

**Mizuki WATANABE**[†a)], **Kazuyoshi UEMATSU**[††], **Sun Woog KIM**[†], **Kenji TODA**[†b)], *and* **Mineo SATO**[††], ***Nonmembers***

**SUMMARY** New $HEu_{1-x}Gd_x(MoO_4)_2$ nanophosphors were synthesized by a simple one-step ion-exchange method. These nanophosphors have rod-like particle morphology with 0.5–15 $\mu$m in length and outer diameters in the range of 50–500 nm. By optimization of the composition, the highest emission intensity was obtained for the samples with $x = 0.50$ for both $KEu_{1-x}Gd_x(MoO_4)_2$ and $HEu_{1-x}Gd_x(MoO_4)_2$.

***key words:*** *Nanophosphor, soft chemical process, rare earth molybdate, layered structure.*

## 1. Introduction

Thin films with dispersed nanophosphor have been investigated for their use in displays, LEDs, and solar cells because of their excellent optoelectronic properties and low light-scattering intensity [1]–[5]. In particular, transparent displays with thin films containing dispersed nanophosphor attracted much attention in the context of next-generation displays [6]. Such transparent displays have been demonstrated mainly in the field of organic light-emitting devices [7]. In addition, stable low-scattering suspensions of inorganic phosphors in organic solvents have to be developed to improve the durability of flexible and transparent displays [8], [9]. However, almost all inorganic phosphors with high luminescence efficiency contain micron-sized particles, which have strong scattering characteristics. The desired insignificant scattering can be obtained for particles smaller than 50 nm [10]. Therefore, nano-sized inorganic phosphors are required for the fabrication of flexible and transparent displays. However, such nanophosphors agglomerate easily in organic solvents. Therefore, the fabrication of stable suspensions of nanophosphors is required.

Several wet chemical methods have been reported for the preparation of nanophosphors, such as the hydrothermal method [11], polymerized complex method [12], sol-gel method [13], and others. These methods offer several advantages, such as homogeneity, phase purity, and narrow size distribution. However, these methods require a special reactor and special precursor materials to achieve complete dissolution in solvent solutions. In addition, methods for the synthesis of clear suspensions of nanophosphors have not been well established until now [14].

In this paper, we propose a new simple synthesis method via ion-exchange for preparing nanophosphors with high luminescence efficiency. We selected a triclinic alkali rare earth molybdate, $KEu(MoO_4)_2$ as the precursor material to synthesize emissive nanophosphors. Triclinic $KEu(MoO_4)_2$ is a well-known phosphor material and presents excellent red emission due to the 4f−4f transition of $Eu^{3+}$ [15]. Furthermore, triclinic $KEu(MoO_4)_2$ has a layered structure, which is shown in Fig. 1, using the VESTA program [16]. In the crystal structure of $KEu(MoO_4)_2$, the polyhedral $EuO_8$ layers are situated between two tetrahedral $MoO_4$ layers along the c-axis with the exchangeable potassium cations located between these $(Eu(MoO_4)_2)_n$ layers. Therefore, the $K^+$ ions in $KEu(MoO_4)_2$ are expected to be exchanged by other ions via ion-exchange methods with corresponding easy control of the particle size and morphology. However, $KEu(MoO_4)_2$ is easily dissolved in concentrated acidic solutions; therefore, there have been no reports on the successful ion-exchange of molybdate and the related synthesis of nanophosphors. On the other hand, we have successfully synthesized $HEu(MoO_4)_2$ nanophosphor with rod-like particle morphology by simple ion-exchange methods in dilute acid, and the solution with the dispersed $HEu(MoO_4)_2$ nanophosphor showed high transparency and strong red-emission due to the f–f transition of $Eu^{3+}$ [17]. In order to further enhance the emission

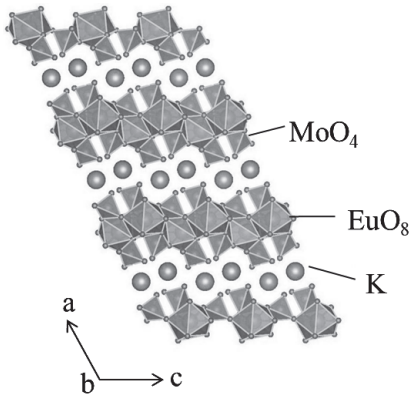


**Fig. 1** Crystal structure of $KEu(MoO_4)_2$.

Manuscript received March 5, 2014.
Manuscript revised June 15, 2014.

[†]The authors are with Graduate School of Science and Technology, Niigata University, 8050 Ikarashi 2-nocho, Niigata 950-2181, Japan.
[††]The authors are with Department of Chemistry and Chemical Engineering, Niigata University, 8050 Ikarashi 2-nocho, Niigata 950-2181, Japan.
a) E-mail: f14k004a@mail.cc.niigata-u.ac.jp
b) E-mail: ktoda@eng.niigata-u.ac.jp

DOI: 10.1587/transele.E97.C.1063

efficiency of $HEu(MoO_4)_2$ nanophosphor, part of the $Eu^{3+}$ ions in the $HEu(MoO_4)_2$ lattice were substituted by smaller $Gd^{3+}$ ions, and the particle morphology and luminescence properties of $HEu_{1-x}Gd_x(MoO_4)_2$ were investigated.

## 2. Experimental

$KEu_{1-x}Gd_x(MoO_4)_2$ ($0.00 \leq x \leq 1.00$) were synthesized by a conventional solid-state reaction method. $K_2CO_3$ (purity 99.95%; Kanto Chemical Co. Inc.), $Gd_2O_3$ (purity 99.99%; Shinetsu Chemical Co. Inc.), $Eu_2O_3$ (purity 99.99%; Shinetsu Chemical Co. Inc.), and $MoO_3$ (purity 99.99%; Kojundo Chemical Co. Inc.) were mixed using a mortar and pestle with acetone; the mixture was then calcined at 700°C for 6 h in air. $HEu_{1-x}Gd_x(MoO_4)_2$ samples were obtained by the $H^+$ exchange of $KEu_{1-x}Gd_x(MoO_4)_2$ in $HNO_3$ solution (0.01 M, 100 mL) at room temperature for 7 days. After stirring, the solutions were isolated by suction filtration using a membrane filter (ADVANTEC MFS, INC., mixed cellulose ester, pore size: 0.45 $\mu$m, diameter: 47 mm). The samples were washed with deionized water for 12 h and then dried at 50°C for 24 h. The obtained $HEu_{1-x}Gd_x(MoO_4)_2$ powder samples were redispersed in deionized water (pH=7).

The obtained samples were characterized by powder X-ray diffraction (XRD, MX-Labo; Mac Science Ltd.) to identify the crystal structure and the sample composition was determined by X-ray fluorescence analysis (XRF, SII, SEA 1200 VX). The sample morphology was characterized by scanning electron microscopy (SEM, Hitachi, S-4300SD). The emission (PL) and excitation (PLE) spectra were measured at room temperature with a spectrofluorometer (Jasco, FP-6500/6600); emission spectra were obtained for excitation at 309 nm, and excitation spectra were obtained for emission at 614 nm.

## 3. Results and Discussion

Figure 2 shows the XRD patterns of the precursor $KEu_{1-x}Gd_x(MoO_4)_2$ ($0.00 \leq x \leq 1.00$) phosphors. The XRD patterns of all samples were in good agreement with single-phase triclinic alkali rare earth molybdate.

Figure 3 shows excitation and emission spectra of the precursor $KEu_{1-x}Gd_x(MoO_4)_2$ ($x$=0.00 and 0.50) phosphors. The excitation spectra of all samples consisted of a strong broad band in the range from 220 to 350 nm, corresponding to the charge-transfer (CT) transition of $O^{2-}$–$Mo^{6+}$. Some strong narrow peaks are observed between 360 and 500 nm and are attributed to the 4f–4f transitions of the $Eu^{3+}$ ion. On the other hand, the CT band of $Eu^{3+}$–$O^{2-}$ is not clearly observed in the excitation spectra, possibly due to the overlap of the CT band with that of the molybdate group [15], [17]–[19]. In the emission spectra, all peaks corresponded to the $Eu^{3+}$ 4f–4f transition. The emission peak intensity corresponding to the $^5D_0$–$^7F_2$ electric dipole transition at 614 nm is higher than that of the $^5D_0$–$^7F_1$ magnetic dipole transition at 592 nm, suggesting that the $Eu^{3+}$

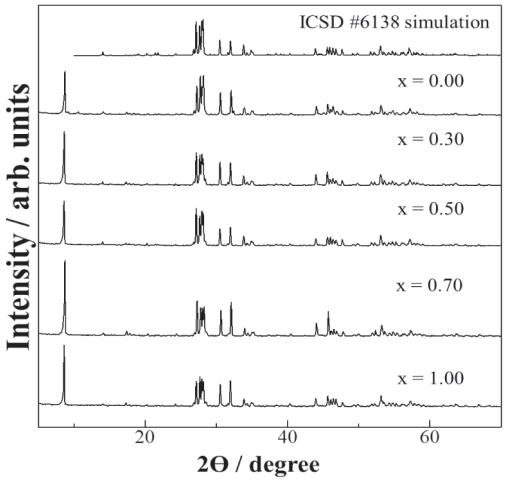


**Fig. 2** XRD patterns of $KEu_{x-1}Gd_x(MoO_4)_2$ ($0.00 \leq x \leq 1.00$) synthesized by the solid-state reaction method at 700°C for 6 h in air.

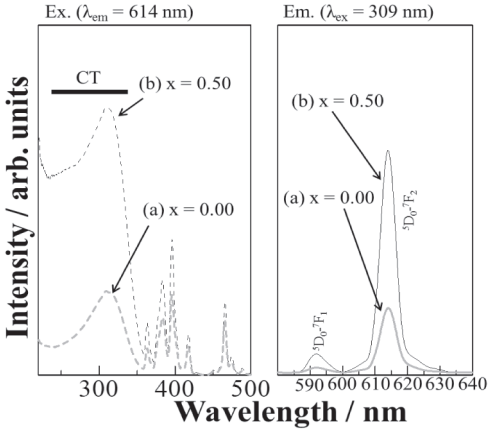


**Fig. 3** Excitation (broken line) and emission (solid line) spectra of $KEu_{1-x}Gd_x(MoO_4)_2$ ($x$=0.00 ((a), gray line) and $x$=0.50 ((b), black line)) phosphors.

ions occupy sites in the $KEu(MoO_4)_2$ lattice without inversion symmetry. The ratio $I_{614\,nm}(^5D_0$–$^7F_2)/I_{592\,nm}(^5D_0$–$^7F_1)$ of $KEu(MoO_4)_2$ (12.5) decreased upon $Gd^{3+}$ doping and was 10.8 in case of $KEu_{0.50}Gd_{0.50}(MoO_4)_2$. This result indicates that the symmetry of the $Eu^{3+}$ site in the $KEu_{1-x}Gd_x(MoO_4)_2$ lattice was higher than that of the sample without the $Gd^{3+}$ doping. It is well known that the $^5D_0$–$^7F_2$ electric dipole transition of $Eu^{3+}$ is sensitively affected by the change of the site symmetry in the host lattice. The peak intensity corresponding to the $^5D_0$–$^7F_1$ transition is relatively higher than that of the $^5D_0$–$^7F_2$ transition when $Eu^{3+}$ is located at a site having high symmetry (inversion symmetry site) in the host lattice, such as in case of $Ba_2GdNbO_5$:$Eu^{3+}$, $NaLuO_2$:$Eu^{3+}$, and $InBO_3$:$Eu^{3+}$ phosphors [20]. Concerning the presently studied $KEu_{1-x}Gd_x(MoO_4)_2$, since the ionic radius of $Gd^{3+}$ (0.1193 nm for 8-fold coordination [21]) is smaller than that of $Eu^{3+}$ (0.1206 nm for 8-fold coordination [21]), a lattice distortion is induced by doping of $Gd^{3+}$ at the $Eu^{3+}$ site of $KEu(MoO_4)_2$, which leads to a change of the local environ-

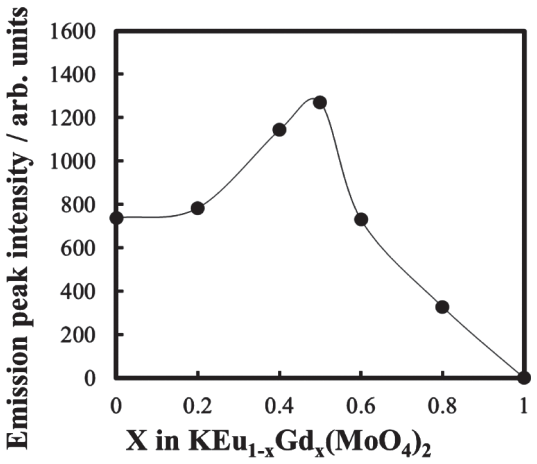


**Fig. 4** Dependence of the emission intensity on the $Gd^{3+}$ content in $KEu_{1-x}Gd_x(MoO_4)_2$ ($0.00 \le x \le 1.00$) phosphors.

ment and symmetry of the $Eu^{3+}$ site in the crystal lattice. On the contrary, the emission intensity of $KEu(MoO_4)_2$ was effectively enhanced by doping of $Gd^{3+}$ into the host lattice. This can be explained by the suppression of the concentration quenching on decreasing $Eu^{3+}$ concentration in $KEu_{1-x}Gd_x(MoO_4)_2$.

Figure 4 shows the compositional dependence of the emission intensity excited at 309 nm of $KEu_{1-x}Gd_x(MoO_4)_2$ ($0.00 \le x \le 1.00$). The emission intensity initially increases with increasing amount of $Gd^{3+}$ and reaches a maximum at $x$=0.50. However, the emission intensity decreases on further increasing $Gd^{3+}$ content beyond the optimum concentration, which is attributed to the decrease of the $Eu^{3+}$ concentration. To synthesize nanophosphors, the obtained $KEu_{1-x}Gd_x(MoO_4)_2$ phosphors were stirred in $HNO_3$ solution at room temperature. However, the $KEu_{1-x}Gd_x(MoO_4)_2$ powders were completely dissolved in highly concentrated $HNO_3$ solution above 0.05 M during the stirring process. In contrast, for the samples stirred in 0.01 M aqueous $HNO_3$ solution for 7 days, the $K^+$ ions of the $KEu_{1-x}Gd_x(MoO_4)_2$ phosphors were successfully exchanged by $H^+$ without particle dissolution. The composition of $KEu_{1-x}Gd_x(MoO_4)_2$ before and after $H^+$ exchange was analyzed by XRF. The amount of $K^+$ ions in the phosphors after $H^+$ exchange was reduced to about 30% compared with the precursor materials $KEu_{1-x}Gd_x(MoO_4)_2$.

To compare the photoluminescence property of $K_{0.3}H_{0.7}Eu_{1-x}Gd_x(MoO_4)_2$ ($H^+$-form) with that of $KEu_{1-x}Gd_x(MoO_4)_2$ ($K^+$-form), the $H^+$-form powders were washed with deionized water for 12 h and then dried at 50°C for 24 h. Figure 5 shows excitation and emission spectra of dried $K^+$-form and $H^+$-form powders. The behavior observed in the excitation and emission spectra of all $H^+$-form powders was similar. The highest emission intensity was obtained for the $H^+$-form with $x$ = 0.50.

The peak wavelength of the CT bands of these phosphors depends on the excitation energy for electron transfer from $O^{2-}$ to $Mo^{6+}$. Since the electronegativity of $H^+$ (2.1)

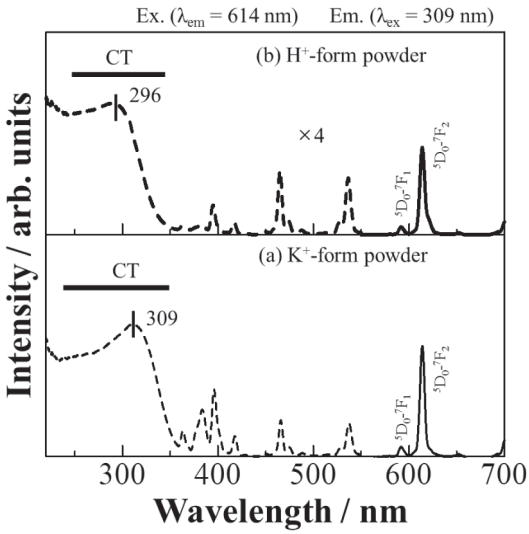


**Fig. 5** Excitation (broken line) and emission (solid line) spectra of dried (a) $KEu_{0.50}Gd_{0.50}(MoO_4)_2$ ($K^+$-form) and (b) $K_{0.3}H_{0.7}Eu_{0.50}Gd_{0.50}(MoO_4)_2$ ($H^+$-form) powders prepared by stirring in 0.01 M $HNO_3$ solution for 7 days.

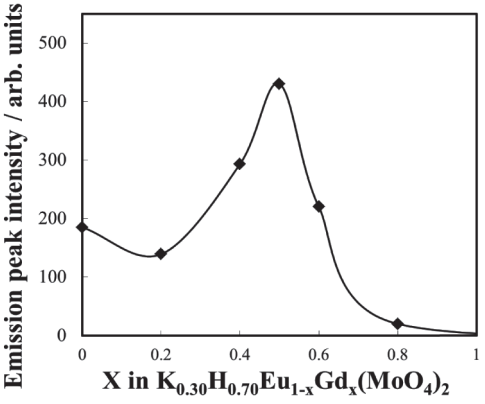


**Fig. 6** Dependence of the emission intensity on the $Gd^{3+}$ content of dried $K_{0.3}H_{0.7}Eu_{1-x}Gd_x(MoO_4)_2$ ($0.00 \le x \le 1.00$) phosphor powders prepared by stirring in 0.01 M $HNO_3$ solution for 7 days.

is larger than that of $K^+$ (0.8), the electronic attractive force between $O^{2-}$ and $Mo^{6+}$ is increased by $H^+$ exchange which, in turn, is causative for the increase of the excitation energy for the electron transfer from $O^{2-}$ to $Mo^{6+}$. As a result, the excitation absorption band corresponding to the CT transition of $O^{2-}$–$Mo^{6+}$ is shifted toward shorter wavelength by $H^+$ exchange. In addition, the peak intensity of the CT transition of $O^{2-}$–$Mo^{6+}$ decreased in comparison with that of the $K^+$-form. This is probably because $H_2O$ persisted in the interlayers as a result of using dilute acid.

Figure 6 shows the compositional dependence of the luminescence intensity excited at 309 nm of $K_{0.3}H_{0.7}Eu_{1-x}Gd_x(MoO_4)_2$ ($0.00 \le x \le 1.00$). Similar to the results obtained for the $K^+$-form samples that are shown in Fig. 4, the emission intensity was effectively enhanced by doping of $Gd^{3+}$ into the $K_{0.3}H_{0.7}Eu(MoO_4)_2$ lattice and the highest emission intensity was obtained for $K_{0.3}H_{0.7}Eu_{0.50}Gd_{0.50}(MoO_4)_2$.

Figure 7 shows SEM images of dried $K^+$-form and $H^+$-

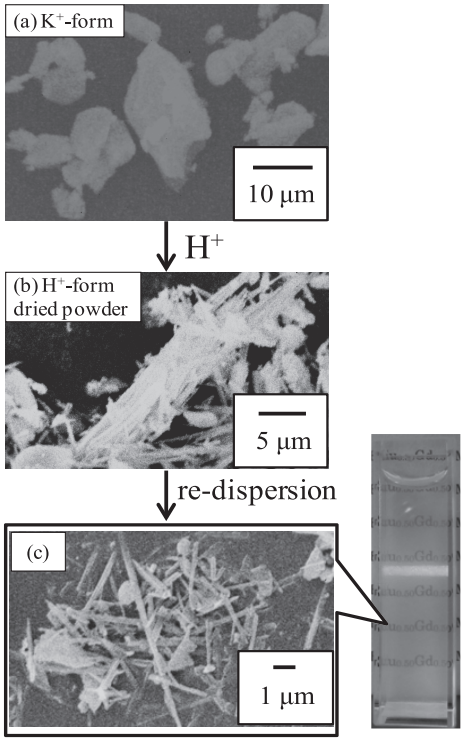


**Fig. 7** SEM images of dried (a) $KEu_{0.50}Gd_{0.50}(MoO_4)_2$ ($K^+$-form) and (b) $K_{0.3}H_{0.7}Eu_{0.50}Gd_{0.50}(MoO_4)_2$ ($H^+$-form) powders and (c) $H^+$-form particles redispersed in deionized water (pH=7) and corresponding photograph of the clear colloidal solution (the concentration of $H^+$-form powder was $1.0 \times 10^{-3}$ mol/dm$^3$).

form powders. The $K^+$-form powder has a granular particle morphology with average particle size of 10 $\mu$m. In contrast, although a small amount of granular particles remained, the dried $H^+$-form powders have rod-like particle morphology with 115 $\mu$m in length and outer diameters in the range of 50–500 nm. These results indicate that the particle size and morphology of $KEu_{1-x}Gd_x(MoO_4)_2$ were successfully changed by $H^+$ exchange at the $K^+$ sites. Although the mechanism of the particle-morphology change remains unexplained in detail, it is possible to consider exfoliation of the $Eu_{1-x}Gd_x(MoO_4)_n$ layers by the substitution of $K^+$ by $H^+$ ions, which may has contributed to the change of the particle morphology. In addition, the rod-like particles formed larger aggregates, like fascicles of fibers. The dispersion of nanophosphors in solution is of high significance for their use in transparent displays. Figure 7(c) shows a SEM image of $H^+$-form powder redispersed in deionized water (pH=7). A corresponding photograph of the suspension after 1 h is also shown in Fig. 7. The concentration of the $H^+$-form powders were adjusted to $1.0\times10^{-3}$ mol/dm$^3$. The Tyndall effect was confirmed by the scattering of a laser beam in the colloidal nanophosphor solution, suggesting that the $H^+$-form nanophosphors were fully suspended in deionized water without precipitation. From Fig. 7(b) and (c), the aggregation of $H^+$-form nanophosphor particles was significantly reduced by the redispersion in deionized water and, as a result, the particles formed small units. These results suggest that $K_{0.3}H_{0.7}Eu_{0.50}Gd_{0.50}(MoO_4)_2$ might be used as a nanophosphor for transparent displays.

## 4. Conclusion

$HEu_{1-x}Gd_x(MoO_4)_2$ nanophosphors were synthesized by one-step ion exchange achieved by stirring $KEu_{1-x}Gd_x(MoO_4)_2$ phosphors in 0.01 M aqueous $HNO_3$ solution at room temperature for 7 days. The obtained $K_{0.3}H_{0.7}Eu_{1-x}Gd_x(MoO_4)_2$ nanophosphors have rod-like particle morphology with 0.5–15 $\mu$m in length and outer diameters in the range of 50–500 nm. The emission intensity of these phosphors was effectively enhanced by $Gd^{3+}$ doping and the highest emission intensity was obtained for the samples with $x$=0.50, both for $KEu_{1-x}Gd_x(MoO_4)_2$ and $K_{0.3}H_{0.7}Eu_{1-x}Gd_x(MoO_4)_2$ phosphors. The aggregated dried nanophosphor powders could be redispersed in deionized water. Thus, it is expected that these phosphors can be applied as a transparent display material.

### References

[1] M. V. Shestakov, V. K. Tikhomirov, D. Kirilenko, A. S. Kuznetsov, L. F. Chibotaru, A. N. Baranov, G. Van Tendeloo, and V. V. Moshchalkov, "Quantum cutting in Li (770 nm) and Yb (1000 nm) co-dopant emission bands by energy transfer from the ZnO nanocrystalline host," Opt. Express, vol.19, no.17, pp.15955–15964, Aug. 2011.

[2] W.-T. Hsu, W.-H. Wu, and C.-H. Lu, "Synthesis and luminescent properties of nano-sized $Y_3Al_5O_{12}:Eu^{3+}$ phosphors," Mater. Sci. Eng. B, vol.104, no.1–2, pp.40–44, Nov. 2003.

[3] Y. Iso, S. Takeshita, and T. Isobe, "Erectrophosretic deposition and characterization of transparent nanocomposite films of $YVO_4:Bi^{3+}$, $Eu^{3+}$ nanophosphor and silicone-modified acrylic resin," Langmuir, vol.30, no.5, pp.1465–1471, Jan. 2014.

[4] A. Potdevin, G. Chadeyron, S. Therias, and R. Mahiou, "Luminescent nanocomposites made of finely dispersed $Y_3Ga_5O_{12}$: Tb powder in a polymer matrix: promising candidates for optical devices," Langmuir, vol.28, no.37, pp.13526–13535, Aug. 2012.

[5] A. Khetubol1, S. Van Snick, A. Hassinen, E. Fron, Y. Firdaus, L. Pandey, C. C. David, K. Duerinckx, W. Dehaen, Z. Hens, and M. Van der Auweraer, "Ligand exchange leads to efficient triplet energy transfer to CdSe/ZnS Q-dots in a poly(*N*-vinylcarbazole) matrix nanocomposite," J. Appl. Phys., vol.113, no.8, pp.083507-1–12, Feb. 2013.

[6] C. W. Hsu, B. Zhen, W. Qiu, O. Shapira, B. G. DeLacy, J. D. Joannopoulos, and M. Soljačić, "Transparent displays enabled by resonant nanoparticle scattering," Nat. Comm., vol.5, no.3152, pp.1–6, Jan. 2014.

[7] S. Choi, S. W. Tae, J. H. Seo, and H. K. Jung, "Preparation of blue-emitting $CaMgSi_2O_6:Eu^{2+}$ phosphors in reverse micellar system and their application to transparent emission display devices," J. Solid State Chem., vol.184, no.6, pp.1540–1544, June 2011.

[8] C. Hilsum, "Flat-panel electronic displays: a triumph of physics, chemistry and engineering," Phil. Trans. R. Soc. A, vol.368, no.1914, pp.1027–1082, Mar. 2010.

[9] V. Bulovic, G. Gu, P. E. Burrows, S. R. Forrest, and M. E. Thomposn, "Transparent light-emitting devices," Nature, vol.380, no.6569, pp.29, Mar. 1996.

[10] V. Buissette, D. Giaume, T. Gacoin, and J.-P. Boilot, "Aqueous routes to lanthanide-doped oxide nanophosphors," J. Mater. Chem., vol.16, no.6, pp.529–539, Oct. 2006.

[11] H. Yang, D.-K. Lee, and Y.-S. Kim, "Spectral variations of nano-sized $Y_3Al_5O_{12}$:Ce phosphors via codoping/substitution and their

white LED characteristics," Mater. Chem. Phys., vol.114, no.2–3, pp.665–669, Apr. 2009.
[12] J. Dhanaraj, R. Jagannathan, T. R. N. Kutty, and C. H. Lu, "Photoluminescence characteristics of $Y_2O_3$:$Eu^{3+}$ nanophosphors prepared using sol-gel thermolysis," J. Phys. Chem. B, vol.105, no.45, pp.11098–11105, Nov. 2001.
[13] H. Hu, L. Xiong, J. Zhou, F. Li, T. Cao, and C. Huang, "Multimodal-luminescence core-shell nanocomposites for targeted imaging of tumor cells," Chemistry, vol.15, no.14, pp.3577–3584, Mar. 2009.
[14] W.-S. Song, H.-N. Choi, Y.-S. Kim, and H. Yang, "Formation of green-emitting $LaPO_4$:Ce,Tb nanophosphor layer and its application to highly transparent plasma displays," J. Mater. Chem., vol.20, no.33, pp.6929–6934, Sept. 2010.
[15] C. Guo, S. Wang, T. Chen, L. Luan, and Y. Xu, "Preparation of phosphors $AEu(MoO_4)_2$ (A=Li, Na, K and Ag) by sol-gel method," Appl. Phys., A Mater. Sci. Process., vol.94, no.2, pp.365–371, Apr. 2009.
[16] R. F. Klevtsova, L. P. Kozeeva, and P. V. Klevtsov, "Preparation and structure of crystals of pottasium europium molybdate, $KEu(MoO_4)_2$," Sov. Phys. Crystallogr., vol.19, no.1, pp.339–355, July 1977.
[17] M. Watanabe, K. Uematsu, S. Kim, K. Toda, and M. Sato, "Nematic liquid crystalline phase of red-emitting $HEu(MoO_4)_2$ nanoscroll," Int. Symp. for Phosphor Materials, Jeju-do, Korea, SO-09, Oct. 2013.
[18] A. Xie, X. Yuan, F. Wang, Y. Shi, J. Li, L. Liu, and Z. Mu, "Synthesis and luminescent properties of $Eu^{3+}$-activated molybdate-based novel red-emitting phosphors for white LEDs," J. Alloy. Comp., vol.501, no.1, pp.124–129, July 2010.
[19] W. L. Feng, Y. Jin, Y. Wu, D. F. Li, and A. K. Cai, "Co-precipitation synthesis and photoluminescence properties of $Ba_{1-x}MoO_4$:$xEu^{3+}$ red phosphors," J. Lumin., vol.134, pp.614–617, Feb. 2013.
[20] T. Kano, "Principal phosphor materials and their optical properties," in Phosphor Hand Book, ed. S. Shionoya and W. M. Yen, pp.178–300, CRC Press, New York, 1999.
[21] R. D. Shannon, "Revised effective ionic radii and systematic studies of interatomic distance in halides and chalcogenides," Acta Crystallogr. A, vol.32, no.5, pp.751–767, Sept. 1976.

**Mizuki Watanabe** is a master-course student at the Graduate School of Science and Technology, Niigata University.

**Kazuyoshi Uematsu** received the Doctoral degree from Niigata University in 2007. He is currently Technical officer of Chemistry and Chemical Engineering, Faculty of Engineering, Niigata University.

**Kim Sun-Woog** received the Doctoral degree from Osaka University in 2012. He is currently Assistant Professor at the Graduate School of Science and Technology, Niigata University.

**Kenji Toda** received the Doctoral degree from Niigata University in 1995. During 1988–1992, he stayed in Nippon Kodoshi Corporation. He is currently Associate Professor at the Graduate School of Science and Technology, Niigata University.

**Mineo Sato** received the Doctoral degree from Osaka University in 1981. He is currently Professor at the Graduate School of Science and Technology, Niigata University.